JOURNAL OF AIRCRAFT
Vol. 48, No. 3, May–June 2011

Estimating Aircraft Fuel Flow for a Three-Degree Flight-Path-Angle Descent

Enis T. Turgut*
Anadolu University, TR 26470 Eskisehir, Turkey

DOI: 10.2514/1.C031260

The objective of this study is to develop statistically significant models in order to determine the effects of altitude on fuel consumption of commercial aircraft during descent for a specific flight-path angle. In this context, the fuel usage trend during descent is investigated for a constant flight-path angle as a function of altitude. For this purpose, flight data records related to ten randomly selected flights are used. To perform the investigation, three model approaches are discussed. In the first method, all descents are evaluated separately. In the second method, all data are evaluated and a general model is established. In the last method, the coefficients found for the models of the first method are examined and a profound relationship is established. For comparative purposes, the results of all approaches are evaluated by statistically determinative indicators and Base of Aircraft Data models. In conclusion, significant relationships between the fuel flow rate and the descent altitude for a 3° flight-path angle are obtained for all models for descents of 70% of the domain. As expected, the best results are found for the first model approach. Standard errors are found between 1.3 and 4.7% of the actual fuel flow rate for corresponding descent altitudes.

I. Introduction

FUEL cost is one of the key direct operating costs for air transport. A variation in fuel price has a direct effect on flight cost. According to International Air Transport Association, the average kerosene price for May 2010 is 88.6 dollars per barrel which corresponds to 708.8 dollars per ton of kerosene [1]. For instance, considering ten flights take place equally over two different relatively short distance routes [five flights per route; the ranges are 345 km (186 n miles) and 463 km (250 n miles)] by B737-800, it is found that the average fuel cost of an entire flight is between 1363–1488 dollars, while the fuel consumption observed only in descent (phase 9) is between 203–251 dollars. Regarding the preceding routes, it can be noted that the proportion of the fuel usage in descent for short distance flights changes between 10 and 24% of the total fuel consumption depending on flight range and aircraft type.

Considering the flight duration and fuel consumption rate, the flight can be split into three parts: climb, cruise and descent. This sequence is also valid for engine power usage, which is high during climb, while low during descent. Regarding flight duration, if the distance between the destination and departure airports allows the aircraft to cruise at their optimum altitude, then the climb and descent phases can each be around 20–30 min. On the other hand, for short distance flights, the descent phase is still significant as shown in the Eurocontrol statement: "The traffic in the European Civil Aviation Conference (ECAC) area is predominantly short haul traffic with nearly half of the flight distance spent in climb or descent phases" [2]. Such a long duration basically highlights the opportunities for fuel savings [3–5].

In this context, a typical mission fuel use according to the flight phases are demonstrated with the flight duration in Fig. 1. Considering three main flight phases, the highest the fuel use is observed in climb, while the lowest is in descent. Furthermore, several more markers can be seen between phases 8 and 9. In addition to the environmental protection, the air traffic management system monitors and regulates the trajectory of a descending aircraft over the air terminal area continuously to eliminate the potential of conflict with the other aircraft performing climb or transit. These regulations sometimes involve maintaining the altitude of aircraft or changing the flight-path angle (FPA) of the descent trajectories and can lead to low-level flight which is not good for fuel consumption. As a result, the markers indicate two low-level flights occurred in this flight. The effect of low-level flight on fuel models is discussed in the section of results and discussion.

During descent, there are variations in engine power due to factors such as adhering to air traffic controller directives, wariness of the minimum height of obstacles in terminal airspace or conditions resulting from weather. In addition to these factors, the effects of the atmosphere pressure should also be noted. Accordingly, during descent the air pressure increases due to the density increase. This allows the lift requirement of the aircraft for the constant thrust to decrease and leads to a decrease in engine power. However, taking into consideration the increase in density, this will also lead to an increase in drag, as well as an extension of the flaps and slats to maintain the FPA by reducing speed and so generating additional drag. Consequently, an increase in engine power is needed as altitude decreases. That is, there is a fuel flow increase resulting from a decrease in altitude.

However, there are some methods which try to reduce fuel consumption in this phase. One of the current procedures aiming to reduce fuel consumption during descent is called continuous descent approach (CDA) procedures, which enable aircraft to track the optimum flight profile using the appropriate FPA. Eurocontrol proposes that the definition of CDA is "an aircraft operating technique in which an arriving aircraft descends from an optimal position with minimum thrust and avoids level flight to the extent permitted by the safe operation of the aircraft and in compliance with published procedures and air traffic control (ATC) instructions" [6].

The most widely-known benefits of CDA procedures are reducing aircraft noise, fuel burn and emissions [7–15]. At present, however, achieving such a cooperative operation of pilots, air traffic controllers and aircraft itself to obtain descent with CDA is quite complex.

Concerning the modeling of fuel consumption as a technical aspect (rather than its correlation with aircraft or fleet selection or route determination, etc. [16–21]), it is difficult to see many examples in the literature. In early 1980s, energy balance algorithm has been used to estimate the fuel consumption of a turbojet engine [3]. Another fuel flow method has been developed by Boeing to calculate the emissions resulted from aircraft [22]. The widely-known NASA emission models have based on these fuel flow models [23,24]. Most recently, the fuel consumption of aircraft in terminal area and in complete mission have been investigated with thrust specific fuel consumption and neural network algorithms, respectively [5,25]. The former is one of the explicit examples that

Received 4 October 2010; revision received 20 December 2010; accepted for publication 20 December 2010. Copyright © 2010 by the American Institute of Aeronautics and Astronautics, Inc. All rights reserved. Copies of this paper may be made for personal or internal use, on condition that the copier pay the $10.00 per-copy fee to the Copyright Clearance Center, Inc., 222 Rosewood Drive, Danvers, MA 01923; include the code 0021-8669/11 and $10.00 in correspondence with the CCC.

*School of Civil Aviation.

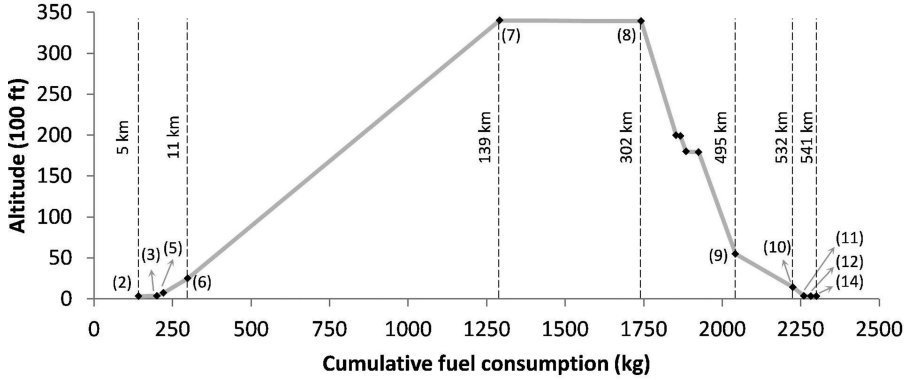

Phase ID	Fuel utilization (%)	Duration (min:sec)
(2) Taxi-out	6.2	10:35
(3) Takeoff	2.5	00:35
(4) Rejected takeoff	NA	NA
(5) Second segment	0.9	00:11
(6) Initial Climb	3.3	00:39
(7) Climb	43.2	11:31
(8) Cruise	19.6	12:15
(9) Descent	13.0	19:19
(10) Approach	8.0	07:15
(11) Final	1.5	01:13
(12) Landing	1.0	00:51
(13) Go-around	NA	NA
(14) Taxi-in	0.8	01:50

Fig. 1 An example for breakdown of fuel uses and corresponding durations of certain flight phases for a B737-800. The location of each number in parenthesis indicates the end of the corresponding phase, while the vertical texts show the distance flown up to the end of this phase.

the actual flight data records (FDRs) have been used. Nevertheless, there is one model which is widely known, called the Base of Aircraft Data (BADA) which should be mentioned. It has been developed by Eurocontrol and covers almost 300 aircraft types [26]. The latest version is labeled as 3.8. In the fuel consumption section of the BADA, the fuel flow function is expressed by three different functions which incorporate the thrust specific fuel consumption as a function of true air speed and equation correction coefficients for all flight phases except cruise and descent idle. During the descent idle and cruise phases, other expressions for fuel consumption apply which are functions of altitude and equation correction coefficients.

The objective of this study is to find a statistically significant relationship between the fuel flow rate and altitude for the descent phase (phase 9: other phases are not considered in this research.) at 3° FPA. For this reason, the B737-800 (hereafter B738) is selected. In addition to the International Civil Aviation Organization aircraft operation document [27], the main reason for using a 3° FPA is that it is a suitable descent angle suggested by a wide range of researchers from the fields of air traffic procedures and aircraft performance [7–9,11]. The originality of this research is that it is based on actual aircraft flight and engine data. Moreover, the modeling aspect is also useful regarding to understanding of the fuel flow trend during descent.

II. Method

For this study, ten domestic flights are randomly selected from a population of all domestic flights of Pegasus Airlines in 2009 for two specific short distance routes. The destination airport is the same for all the flights (Istanbul Sabiha Gokcen Airport, Turkey), while the departure airports are Antalya Airport (LTAI) for the first five flights (denoted as F1 through F5) and Izmir Airport (LTBJ) for the second five flights (denoted as F6 through F10). Istanbul Sabiha Gokcen Airport (LTFJ) is located 35 km southeast of Istanbul. LTFJ has a single runway which is oriented 06/24 and the dominant arrival patterns are the direction to runway 06. According the traffic volume LTFJ is the second largest airport in Istanbul Terminal Airspace. The airport served 6.6 million passengers and more than 60,000 aircraft movements in 2009. The locations are given in Table 1.

These flights were performed by the same type of aircraft (but not aircraft of the same tail number) and engines. The aircraft type considered is the B737-800, which is a twin-engine short-to-medium-range aircraft. The engine type used in these aircraft is the CFM56-7B, a high-bypass turbofan engine with a bypass ratio of 5.5, an overall pressure ratio of 32, and a thrust rating of 115 kN. Actual data on fuel flow, aircraft speed, engine speed ($N1, N2$), altitude, aircraft mass and so on are obtained from aircraft FDRs.

Processing the FDR is not easy since there may be anomalies related to observations which are recorded at 1 s or even three or four times per second. These anomalies are caused by the instantaneous reaction of the electronic engine computer (EEC) of full authority digital engine control system to condition variations such as autopilot commands, throttle, air traffic directives, altitude, ambient temperature and pressure, bleed air usage, anti-ice air usage and so on. Since, the time interval of saved observations is so small it is usual to see these anomalies in the records. Therefore, building models based on these observations might generally not allow the establishment of a regular or significant model and necessitate the filtering of noise data from the records. The ratio of the filtered data is provided at the subsequent section.

There are many factors that can affect fuel consumption during a flight. Among these factors, are weight, weather conditions, air traffic management, and company policy in terms of cost index and so on. Therefore, even considering the same routes and the same aircraft, it would be exceptional to observe identical fuel consumption. In this context, in order to reduce fuel consumption, airline companies implement certain procedures such as not carrying unnecessary items (excessive fuel, excessive baggage, food, reading material, and suchlike), reducing the operating time of engine on the ground, single

Table 1 Aerodrome locations

Aerodrome location indicator and name	Aerodrome reference point coordinates
LTFJ: Istanbul Sabiha Gokcen (Int.)	405354N 0291833E
LTBJ: Izmir Adnan Menderes (Int.)	381721N 0270918E
LTAI: Antalya (Int.)	365401N 0301734E

Table 2 Flight information of ten random flights[a]

ID	Flight date	Arrival time	Flight duration, min	Load factor	Payload, kg	Fuel on board (top of descent)/fuel on board (takeoff), kg	Mass (top of descent)/mass (takeoff), t
F1	30 Dec. 09	11:56	67.2	0.69	1475	3765/5434	58.08/59.67
F2	29 Dec. 09	09:05	66.5	0.37	617	3375/4944	51.85/53.47
F3	27 Dec. 09	18:52	66.7	0.76	694	3611/5098	58.42/60.13
F4	26 Dec. 09	06:26	64.7	0.53	776	3765/5407	55.01/56.70
F5	25 Dec. 09	12:02	73.8	0.83	1144	3579/5221	60.07/61.80
F6	26 Dec. 09	09:47	64.9	0.66	767	3801/5103	56.92/58.24
F7	22 Dec. 09	19:22	64.2	0.64	754	4105/5393	56.86/58.19
F8	12 Sept. 09	19:13	54.6	0.84	3190	4055/5416	62.63/64.08
F9	12 Aug. 09	09:25	52.9	0.75	1095	3788/5144	56.35/57.75
F10	12 June 09	06:33	48.2	0.73	895	3846/4999	58.62/59.86

[a]Regular capacity of B738 is 189 passengers. Payload includes baggage and cargo.

engine taxiing, rational fuel management and so on. Flight information is given in Table 2.

In the analysis part, data regarding the descent parts where a 3° FPA (±0.25°) is gathered. Since, standard arrival route procedures do not exist (in 2009) for Sabiha Gokcen Airport, descent procedures can be observed at different vertical profiles (see Fig. 2). Therefore, the applied FPAs may be different descent by descent. The variations of the FPA of ten descents are given in Table 3. From table, it can be seen that relatively higher FPAs are used in F4, F8 and F9, while lower FPAs are observed for descents of F6, F7 and F10.

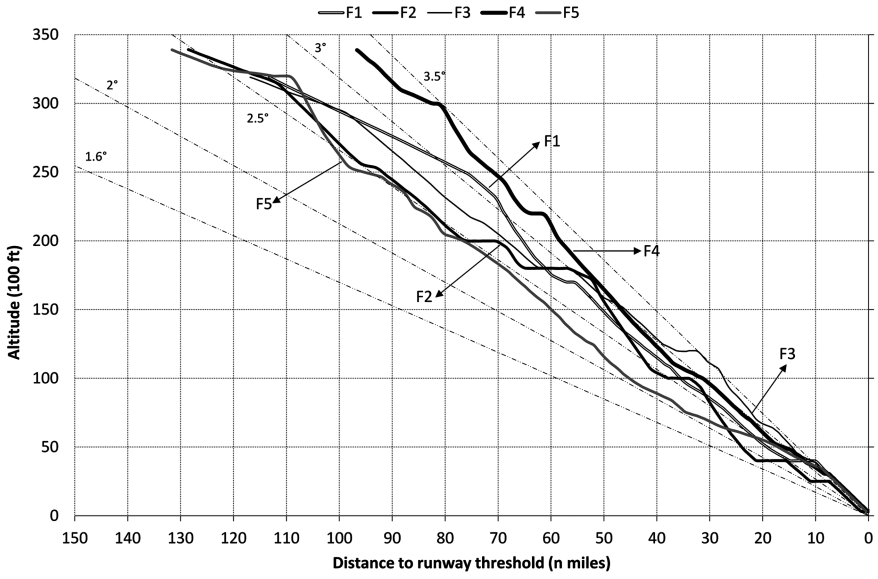

a)

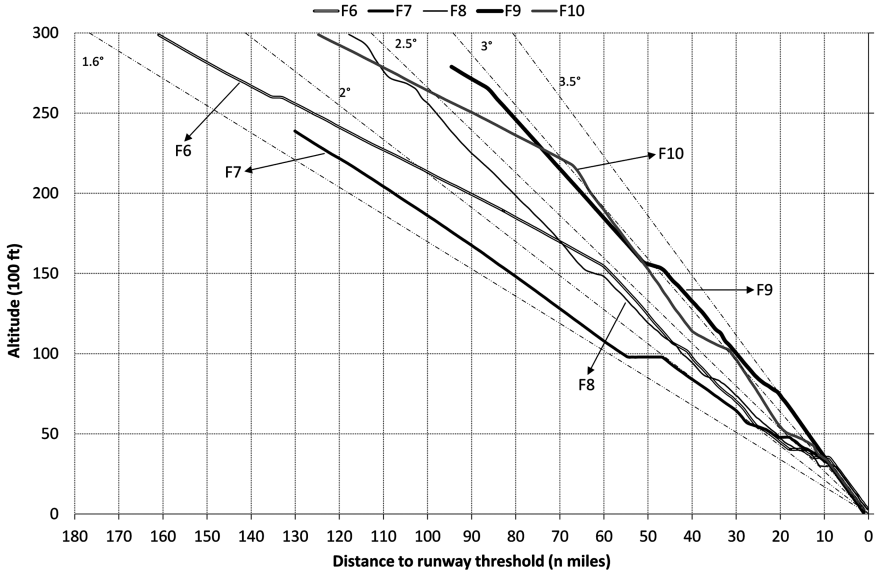

b)

Fig. 2 Descent vertical profiles of aircraft departing from a) Antalya and b) Izmir airports.

Table 3 The breakdown of used FPAs during descent

ID	Data count	Flight-path angle, %[a]													
		0.5°	1.0°	1.5°	2.0°	2.5°	3.0°	3.5°	4.0°	4.5°	5.0°	5.5°	6.0°	6.5°	7.0°	7.5°
F1	1124	1	1	19	27	9	16	14	6	1	2	2	1	1	0	0
F2	964	4	5	19	6	7	12	15	4	2	9	10	3	1	0	1
F3	943	1	7	17	8	6	31	17	6	3	2	0	0	1	1	0
F4	919	1	3	11	7	6	15	23	19	4	2	2	3	3	1	0
F5	1348	7	14	20	16	13	9	8	3	2	2	1	1	2	1	0
F6	1329	1	9	61	7	8	12	3	0	0	0	0	0	0	0	0
F7	1124	2	5	37	53	1	1	1	0	0	0	0	0	0	0	0
F8	1089	3	8	10	14	32	25	5	2	1	0	0	0	0	0	0
F9	805	2	3	13	6	11	56	7	0	0	1	0	0	0	0	0
F10	1087	0	18	41	2	1	5	15	13	3	0	0	0	0	0	0

[a]FPAs are determined with an allowed range of ±0.25°.

As can be seen from Table 3, the descent portion with a 3° FPA is different for each descent. Furthermore, it should be noted that the altitude region for these portions is also different for each descent.

III. Results and Discussion

In this section, an investigation is carried out to ascertain if there is a single model that could cover for all ten descents. To perform this task, all of the descents are first examined individually to note any relationship between fuel flow rate and altitude. Subsequently, the individual models found for each descent are evaluated to see if the possibility exists to develop a single model that could be relevant for all descents. The validation for models is conducted by three statistical parameters: coefficient of determination, standard error and F significance (F sig.).

It should also be noted that the fuel flow rates or other parameters, such as altitude and engine speeds are obtained from the FDR for a single engine. Although the parameters of both engines (left and right engines) are mostly equal some differences can be observed due to the characteristics of engines, but they are too small to be considered. Therefore, unless otherwise stated the results are given for individual engines. However, the results for aircraft can be easily found by doubling the outputs found for one of the engines. Apart from that, although the SI units are used throughout the study, for the sake of simplicity with the FDRs, the unit for altitude is given in feet.

A. Models Based on Individual Descent

Firstly, all descents are investigated individually in order to observe if a tangible relationship exists between fuel flow rate and altitude. At this point, in order to maintain the standard error as low as possible, the noise data is filtered. The requirements of the filtering process resulted from the EEC commands on the fuel control unit (FCU). To maintain the required fuel air ratio in respect of the all the engine power settings, and aircraft attitude (not altitude), weather conditions, use of the engine bleed air and so on, the EEC continuously monitors fuel flow and controls the FCU. The flight conditions, or change in bleed air requirements due to the air conditions of the cabin or internal air system of the engine might lead instant and relatively large (or unusual) deviations in the fuel flow data. These deviations normally only last for a small duration (in the order of several seconds) but are recorded by the EEC to FDR while it has an impact on the model. To overcome this inconvenience, these deviations are removed (filtered) from the data.

The ratios of the filtered data to the data count of a 3° FPA are given in Table 4. As can be seen from the table, the regular 3° FPA data count is considerably lower than the total descent data count which is given in Table 3. This also indicates the percentage of use of a 3° FPA for the entire descent. In the last column of Table 4, the altitude regions are also shown. Accordingly, except for the descents of F3 and F7, it can be seen that reasonable vertical regions are travelled by the remaining descents at a 3° FPA.

According to the correlation and regression analyses, except for one descent, a linear relationship between fuel flow rate and altitude is established with significantly low standard errors as follows:

$$y = i + xh \tag{1}$$

where y and h stand for fuel flow rate ($\text{kg} \cdot \text{h}^{-1}$) and altitude (ft), while i and x denote the intercept and variable of the function.

The statistical parameters are tabulated in Table 5. As it shows a heavily fluctuating trend, no significant model can be found for F3 and therefore, is removed from the domain. For the remaining descents, the linear relationships between fuel flow rate and altitude indicate an increase in fuel flow rate of 7–15 $\text{kg} \cdot \text{h}^{-1}$ for every 305 m (1000 ft) decrease in descent.

In Fig. 3 several examples regarding the fitness of individual models are shown with solid black lines for the descents of F2, F5, F8 and F9. These descents are selected as they provide the least and highest standard errors and have higher data counts. From Table 5, it can be clearly seen that the intercept and slope of F2 and F5 are higher than those for F8 and F9. The main reason for this difference can be attributed to the difference of vertical regions where the 3° FPA is observed and the frequency and duration of the use of the 3° FPA. Since the power settings can be different for each FPA, switching from one FPA to another would require some time for stabilizing the parameters for new FPA. When the frequency of these switches is

Table 4 Information regarding descents at a 3° FPA

ID	Total data count	Filtered data count	Filtered data ratio, %	Altitude region (100 ft)
F1	70	66	5.7	187-69
F2	112	108	3.6	305-94
F3	68	50	26.5	319-295
F4	138	124	10.1	312-45
F5	123	90	26.8	254-108
F6	155	154	0.6	152-55
F7	15	15	0.0	63-58
F8	275	182	33.8	292-112
F9	451	445	1.3	261-86
F10	56	49	12.5	215-53

Table 5 Information regarding the model and statistical parameters for a 3° FPA for all descents

ID	Model	R^2	Std. err., $\text{kg} \cdot \text{h}^{-1}$	F sig.
F1	$425.48 - 9.2 \times 10^{-3}h$	0.98	4.2	3.96×10^{-53}
F2	$545.35 - 12.8 \times 10^{-3}h$	0.89	19.9	2.82×10^{-53}
F3[a]	——	——	——	——
F4	$412.22 - 8.2 \times 10^{-3}h$	0.98	9.5	4.4×10^{-110}
F5	$663.51 - 14.9 \times 10^{-3}h$	0.96	10.7	1.38×10^{-65}
F6	$429.15 - 9.2 \times 10^{-3}h$	0.98	3.9	5.40×10^{-124}
F7	$453.40 - 13.4 \times 10^{-3}h$	0.75	1.5	3.12×10^{-5}
F8	$408.70 - 7.3 \times 10^{-3}h$	0.98	5.2	2.60×10^{-150}
F9	$408.30 - 7.8 \times 10^{-3}h$	0.99	4.5	0
F10	$428.18 - 9.0 \times 10^{-3}h$	0.98	6.3	3.12×10^{-42}

[a]F3 is excluded from the domain as its data fluctuates substantially. h and R^2 denote altitude (ft) and coefficient of determination, respectively.

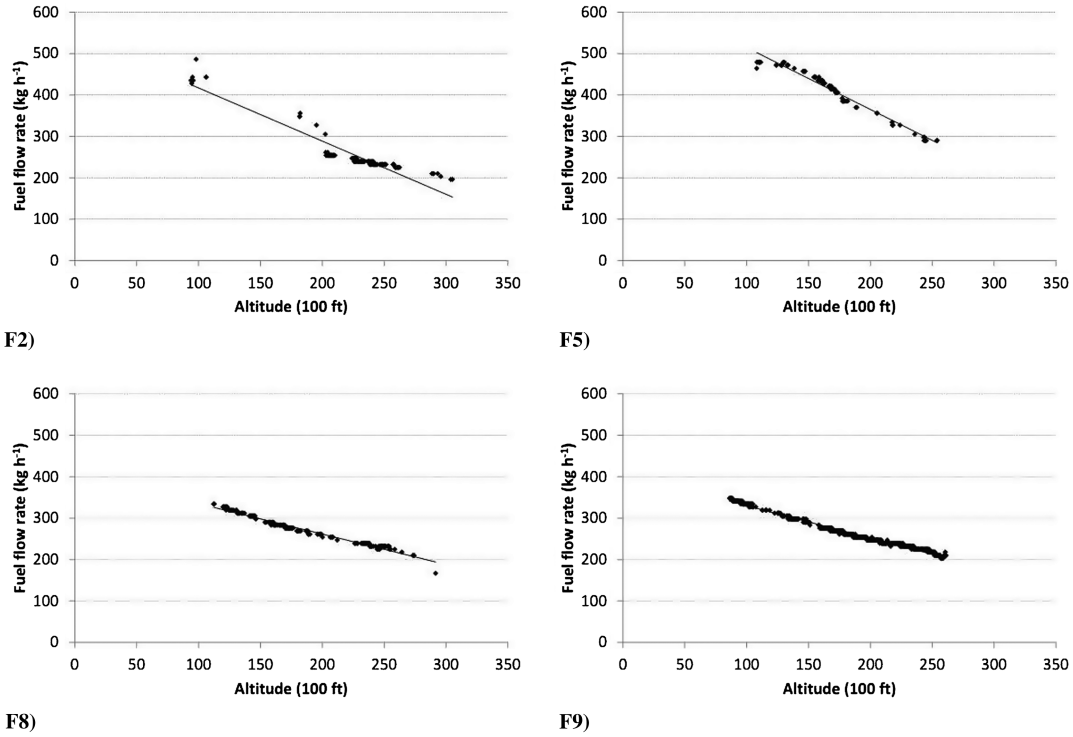

Fig. 3 Examples for fitness of individual models.

high or the duration of tracking an FPA is low this has a negative effect on the trend of parameters, not only the fuel flow rate, but also other parameters, such as engine speeds ($N1$ and $N2$).

This effect can be seen in Fig. 4. According to the frequency of the descent, it can be seen that there are 3° FPA groupings at certain altitude intervals for F2 and F5 compared with a more uniformly distributed use of 3° FPA for F8 and F9. This implies the aircraft follow a 3° FPA track at a reasonable time but only for a limited altitude region for F2 and F5. For instance, in the descent of F2, an accumulation of a 3° FPA use is observed between 6096–7925 m (20,000–26,000 ft), while a similar use occurred under 5486 m (18,000 ft), however, with a relatively low frequency for the descent of F5. On the other hand, regarding engine speed for these descents, small but important differences appeared as the average $N1$ speeds of 36, 38, 33 and 33% for F2, F5, F8 and F9, respectively.

Apart from this, from Table 5, it can be seen that the slope of F7 also appears higher compared with other regular descents (all descents excluding F2 and F5). This difference results from the relatively low data count observed in F7. However, despite the low data count, a similar linear relationship between fuel flow rate and altitude is established.

It is obvious that the difference observed for F2 or F5 has an impact on the development of general models. However, although the use of a 3° FPA for these flights is not ideal compared with the other regular descents, the linear relationship between fuel flow rate and altitude is still accepted as sufficiently significant in terms of the fitness of the model. This also implies another important result that is the effect of the frequency of the FPA switch on fuel flow during descent.

B. General Model Based on All Descents

In this section, a general model that could be available for the given individual models is developed. To do this, two methods are investigated. In the first method the data of all nine descents are analyzed together. F3 is excluded from the analysis domain for the preceding reason. Furthermore, F2 and F5 are also excluded from the domain since their intercept coefficients are relatively different than the other descents, leading to a substantial deviation to the fitness of the model. The characteristic of the deviation is also reported by certain statistical parameters.

In the second method, the coefficients of the individual model are investigated separately as intercept and variable as if there is a further

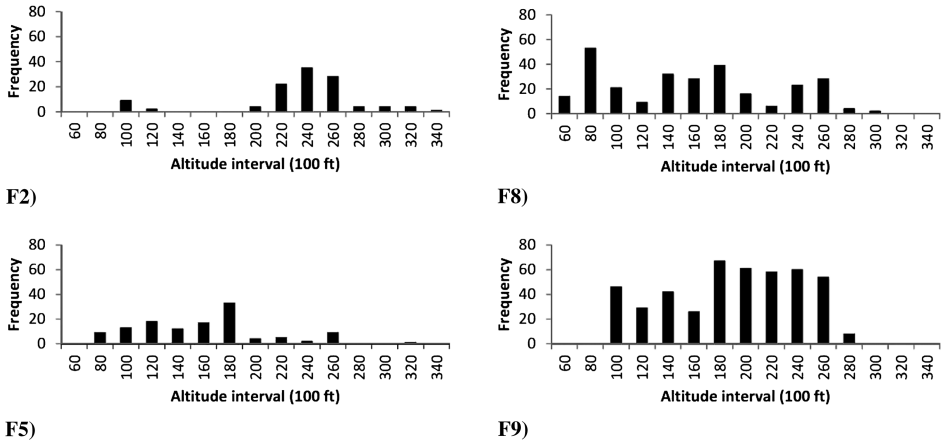

Fig. 4 The histogram of vertical regions where a 3° FPA is tracked. Frequency denotes data count.

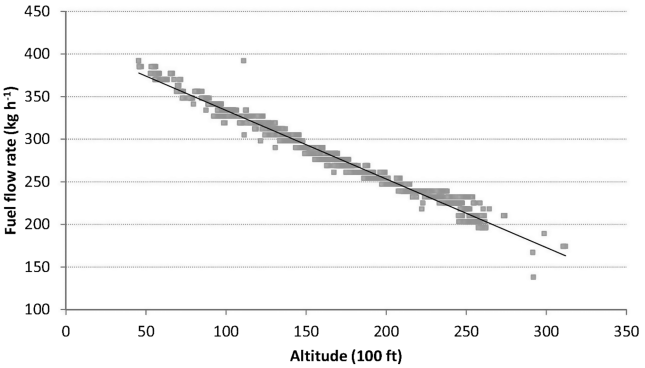

Fig. 5 The fitness of general model based on data of all seven descents.

relationship between the intercept and variables with altitude. In the following subsections, the results are discussed.

1. General Data Analysis

As can be seen from Table 5, there are seven descents where the intercept and variable coefficients are similar. This provides motivation regarding a similar relationship between fuel flow rate and altitude which could exist for all seven descents.

A regression analysis is applied to a total of 1035 data pairs (altitude and corresponding fuel flow rate). As a result, a significant relationship is established. The model result is calculated as

$$y = 414.30 - 8.1 \times 10^{-3} h \tag{2}$$

and the statistical outputs, R^2 (coefficient of determination), standard error and F sigs. are found to be 0.98, 7.3 and ∼0, respectively. The fitness of Eq. (2) is illustrated in Fig. 5. The model suggests that each 305 m (1000 ft) of decrease in altitude leads to an increase in fuel flow rate at around 8.1 $\text{kg} \cdot \text{h}^{-1}$.

Although the model is appeared to be significant for seven descents, performing a comparison against to the individual models could be advisable. This comparison is illustrated in Fig. 6. According to the data, considering the standard errors of individual models, it can be seen that none of the descents present a better standard error for the model obtained by Eq. (2). The average of standard errors for individual models is 5.0 $\text{kg} \cdot \text{h}^{-1}$, while it is 7.8 $\text{kg} \cdot \text{h}^{-1}$ for the standard errors obtained by Eq. (2). Indeed, the difference exceeds four fold of standard error for F7 and two fold of standard error for F8. However, although the results obtained by Eq. (2) are worse than those for the individual models, considering the actual fuel flow rates, it is worth noting that the average standard errors for both model approaches provide very small errors at 1.3–4.7% of the actual fuel flow rates.

2. Coefficient Analysis

In this section, in order to achieve a general model, the reasons for the intercept and the variable variations at each descent are investigated. Firstly, strong relationships between coefficients and altitude are found through the scattered diagram. This could be attributed to the different vertical regions that the trajectory of 3° FPA

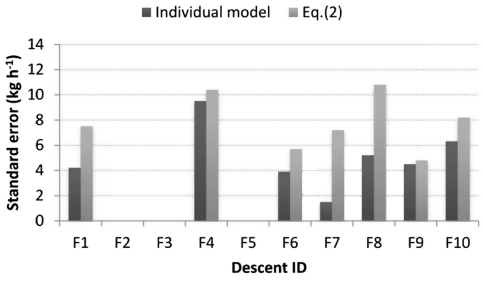

Fig. 6 Standard error comparison for two different model approaches in terms of fuel flow rate.

Table 6 Tabulated intercept and variable values of seven descents

ID	Top altitude, ft	Bottom altitude, ft	Intercept	Variable
F1	18,720	6968	425.48	-9.2×10^{-3}
F2[a]	——	——	——	——
F4	31,203	4543	412.22	-8.2×10^{-3}
F5[a]	——	——	——	——
F6	15,193	5516	429.15	-9.2×10^{-3}
F7	6338	5764	453.40	-13.4×10^{-3}
F8	29,159	11,225	408.70	-7.4×10^{-3}
F9	26,133	8620	408.30	-7.8×10^{-3}
F10	21,471	5337	428.18	-9.1×10^{-3}

[a]F2 and F5 are excluded from domain as their intercepts are different from other descents.

is used for each flight. Based on these relationships, two regression analyses are performed separately for intercept altitude and variable altitude. The required values for the analysis are tabulated in Table 6.

The linear relationship between the intercepts of seven descents and altitudes where a 3° FPA is tracked suggests a correlation coefficient of 0.95 between the top altitudes and the intercepts. Regarding the regression analysis, the model for the intercept (i) of the fuel flow rate function can be given as a function of altitude as follows:

$$i = 460.61 - 0.00175h \tag{3}$$

Of the statistical parameters for Eq. (3), R^2, the standard error and F sig., which indicate the significance of the model are found to be 0.90, 5.5 and 0.0011, respectively.

On the other hand, a nonlinear relationship between the variables of seven descents and altitudes is established with a correlation coefficient of 0.97. The output of the regression analysis suggests a model for the variable (x) of the fuel flow rate function [in Eq. (1)] as follows:

$$x = 3.32 \times 10^{-16} h^3 - 2.90 \times 10^{-11} h^2 + 9.19 \times 10^{-7} h - 0.01807 \tag{4}$$

where R^2, the standard error and F sig. are calculated as 0.95, 6.22×10^{-4} and 0.018, respectively. Therefore, according to the statistical indicators, a strong relationship between the coefficients and altitude is observed. Investigation shows there are other parameters in addition to altitude, could have an effect on coefficients; aircraft mass and ground speed are also examined. However, no evidence is found which could indicate such a relationship exists.

Once the functions (i and x) for the coefficients are found, in order to measure the fitness, a test process is applied to the data through the use of functions as follows:

$$y = 460.61 - 0.00175h + (3.32 \times 10^{-16} h^3 - 2.90 \times 10^{-11} h^2 + 9.19 \times 10^{-7} h - 0.01807)h \tag{5}$$

and the results for the descents having the lowest and the highest standard error are demonstrated in Fig. 7.

In Fig. 7, it can be seen that the error calculated for F8 is between 0 and 20 $\text{kg} \cdot \text{h}^{-1}$, while it is between −10 and +10 $\text{kg} \cdot \text{h}^{-1}$ for F9. Furthermore, the highest errors occurred at the highest and lowest altitudes. The main reason that could be attributed to this trend is the change in the configuration of the aircraft. Accordingly, when the aircraft initiates a descent, a gradual decrease in engine power settings is observed instead of a sudden decrease. For example, in F2, the averaged cruise $N1$ and $N2$ speeds are 83 and 90%, respectively. However, beginning with the last 12 s of the cruise phase, the $N1$ and $N2$ speeds starts a gradual decrease. These speeds are observed as 72 and 85% in the beginning of the descent phase. For a comparison purpose, the cruise $N1$ and $N2$ speeds (79 and 90%, respectively) of F9 starts to decrease 38 s before the switching to the descent phase. The $N1$ and $N2$ speeds at the start of descent phase are observed as 44

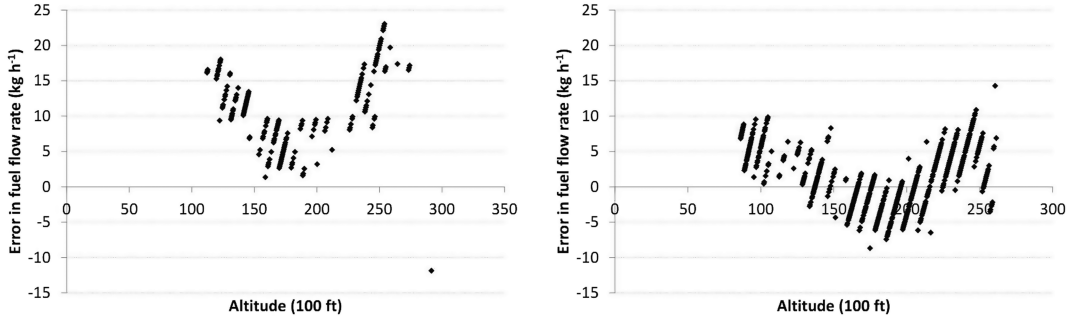

Fig. 7 The errors in fuel flow rate obtained using Eq. (5) for a) F8 and b) F9. For the display simplicity, one of spurious data (error of −40.6 kg · h^{-1} at 29,197 ft) is removed from the graphic (a).

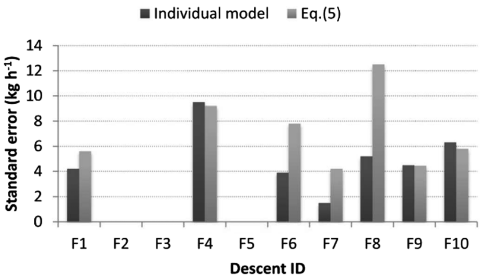

Fig. 8 Standard error comparison for two different model approaches in terms of fuel flow rate.

and 80%, respectively. Therefore, the aircraft might require a reasonable amount of vertical region to stabilize the engine power settings for descents. This vertical region could depend on the time schedule, weather or air traffic directives. A similar circumstance is valid when the aircraft is at low altitudes, since at this time the final approach arrangements in terms of flight control surfaces could set for landing or the air traffic controller directives resulting from traffic or terminal air space obstacles might lead the aircraft to change its regular flight path.

In Fig. 8, a standard error comparison is illustrated for the individual models for each descent (the black bar) and the model developed by Eq. (5) for all seven descents. It is clear from to the chart that, in general, the standard error of individual models is found to be lower than those for Eq. (5) and also the amount of difference of the standard error is in favor of the individual models. Only for the descents of F4 and F10, are the standard errors found by Eq. (5) to be lower than those for individual models, while the standard error of F9 is found to be almost the same for both model approaches. Nonetheless, since the average standard error of the results of Eq. (5), i.e., 7.1 kg · h^{-1}, is lower than those for Eq. (2), the upper limit of the error percentage against the actual fuel flow rates is decreased from 4.7 to 4.2%.

At the end of the discussion, a final remark should be given to the BADA model. According to the theoretical descent data of a B738 at nearly constant FPA (i.e., ∼3°) from 12,500 to 915 m (41,000 to 3000 ft), the relationship between fuel flow rate and descent altitude is obtained as follows:

Table 7 Records regarding to low-level flights during descent

Flight ID	Altitude (100 ft)	Duration, s	Average fuel flow rate, kg · h^{-1}
F2	200	52	521
F2	180	91	800
F3	180	42	497
F3	120	32	565
F5	322	84	845

$$y = 429.75 - 6.8 \times 10^{-3} h \quad (6)$$

It is also note to worth that the Eq. (6) provides good values for R^2, the standard error and F sig. as 0.99, 1.0 and 6.27×10^{-38}, respectively. In addition, considering the coefficients of Eq. (2) or separate models, it can be seen that certain differences appeared for both variables. Nevertheless, these differences could be attributed mainly to the mass of the BADA sample aircraft (i.e., 65.3 t) and the zero wind condition that is accepted by the BADA model. However, the differences of coefficients appear to be reasonably low and it is believed that a good consistency between the BADA and suggested models is provided.

C. Error Analysis

In addition to high rate of data fluctuation in F2, F3 and F5, there is another reason which could be attributed to the failure to develop a relationship between fuel flow and descent altitude. It is indicated from the flight records that all of the three flights are performed low-level flights during the phase of descent (switching to phase 8 during phase 9 at relatively short intervals). This leads to a change in the configuration of the aircraft depending on the altitude, thereby the fuel flow rate. Low-level flights occurred during descent are given in Table 7 for these three flights. These are also evident from the vertical profiles given in Fig. 2. This kind of low-level flight which requires phase switching is not observed for other flights.

Considering the fuel flow rate obtained from the models, it can be seen from Table 7 that the average fuel flow rates are higher than those for performing regular descent resulting a change in fuel flow trend. Since this paper only focuses about the fuel flow trend at 3° FPA, one may note that the failure on models peculiar to these flights should not be attributed to the low-level flights. However, according to the FDR, there are evidences related to occurrence of descent at 3° FPA subsequent of low-level flights. Therefore, it is reasonable to consider the negative effects of low-level flight on fuel flow model efforts.

IV. Conclusions

One of the key concerns of mitigation strategies for the environmental impact of aircraft and the fuel consumption of air transport is the implementation of an efficient air traffic management system. Holding an aircraft over an airport for 15–20 min can simply eliminate a substantial part of the technological achievements obtained for either fuel economy or environmental issues.

Despite having relatively lower engine power settings, descent is as a phase which could possess good potential for fuel savings and emissions mitigation using efficient air traffic management. In this context, investigations have shown that rather than a conventional stair-step descent, a CDA could yield better fuel consumption and emission characteristics as it provides almost constant and relatively low engine power settings throughout the descent.

Motivated by an efficient fuel consumption requirement, in this study the relationship between fuel flow rate and altitude during the

phase of descent at a 3° FPA is analyzed. The search domain is composed of ten randomly selected B737-800 commercial aircraft. To process the fuel consumption trend, the actual flight data are used. The relationship analysis involves both separate and general examinations of the descent data. A comparison is also made for the results found for different examinations. As a result, the investigation has shown that there is a good relationship between fuel flow rate at a 3° FPA and altitude during descent which could be mathematically modeled. It is also concluded that the suggested models peculiar to each descent are found to be significant for 90% of the domain, while general models are found to be significant for 70% of the domain. Models also provide low standard errors at between 1.3–4.7% of actual fuel flow rates. Any significant model could not be established for the rest of the domain due to high data fluctuation rates, high frequency of FPA changes and the low-level flights at cruise configurations.

Acknowledgments

The author would like to thank Mustafa Kemal Helvacioglu (Safety Manager), Cahit Tasbas (Training Manager), and Flight Data Monitoring Specialist Sercin Ozen (Flight Safety Department) from Pegasus Airlines for their sincere cooperation in the study. Thanks should also be given to Oznur Usanmaz from the Department of Air Traffic Control, Anadolu University, for her kind assistance in data acquisition.

References

[1] "Kerosene Price," http://www.iata.org/whatwedo/economics/fuel_monitor/Pages/index.aspx [retrieved 15 May 2010].

[2] European Organization for the Safety of Air Navigation, "Eurocontrol Manual for Airspace Planning," Vol. 2, Eurocontrol, Brussels, 2003, pp. 4–2.

[3] Collins, B. P., "Estimation of Aircraft Fuel Consumption," *Journal of Aircraft*, Vol. 19, No. 11, 1982, pp. 969–975.

[4] Pant, R., and Fielding, J. P., "Aircraft Configuration and Flight Profile Optimization Using Simulated Annealing," *Aircraft Design*, Vol. 2, No. 4, 1999, pp. 239–255. doi:10.1016/S1369-8869(99)00020-8

[5] Senzig, D. A., Fleming, G. G., and Iovinelli, R. J., "Modeling of Terminal-Area Airplane Fuel Consumption," *Journal of Aircraft*, Vol. 46, No. 4, 2009, pp. 1089–1093. doi:10.2514/1.42025

[6] Eurocontrol, "Continuous Descent Approach: Implementation Guidance Information," www.eurocontrol.int/environment, [retrieved 25 April 2010].

[7] Wubben, F. J. M., and Busink, J. J., "Environmental Benefits of Continuous Descent Approaches at Schiphol Airport Compared with Conventional Approach Procedures," National Aerospace Lab. NLR-TP-2000-275, 2000.

[8] Anderson, L. R., and Warren, A. W., "Development of an Advanced Continuous Descent Concept Based on a 737 Simulator," *Proceedings. The 21st, Digital Avionics Systems Conference, 2002*, Vol. 1, 2002, pp. 1E5-1–1E5-4.

[9] Warren, A., and Tong, K., "Development of Continuous Descent Approach Concepts for Noise Abatement (ATC)," *Proceedings. The 21st, Digital Avionics Systems Conference, 2002*, Vol. 1, 27–31 Oct. 2002, pp. 1E3-1–1E3-4.

[10] Clarke, J. P. B., Ho, N. T., Ren, L., Brown, J. A., Elmer, K. R., Tong, K., and Wat, J. K., "Continuous Descent Approach: Design and Flight Test for Louisville International Airport," *Journal of Aircraft*, Vol. 41, No. 5, 2004, pp. 1054–1066. doi:10.2514/1.5572

[11] Weitz, L. A., Hurtado, J. E., Barmore, B. E., and Krishnamurthy, K., "An Analysis of Merging and Spacing Operations with Continuous Descent Approaches," *24th Digital Avionics Systems Conference*, Vol. 1, 2005, pp. 2.C.3-1–2.C.3-11.

[12] Wilson, I., and Hafner, F., "Benefit Assessment of Using Continuous Descent Approaches at Atlanta," *24th Digital Avionics Systems Conference*, Vol. 1, 2005, pp 2.B.2–2.1-7.

[13] Callantine, T. J., Palmer, E. A., Homola, J., Mercer, J., and Prevot, T., "Agent-Based Assessment of Trajectory-Oriented Operations with Limited Delegation," *25th Digital Avionics Systems Conference*, IEEE/AIAA, Portland, OR, 2006, pp. 1–11.

[14] Alam, S., Nguyen, M. H., Abbass, H. A., Lokan, C., Ellejmi, M., and Kirby, S., "A Dynamic Continuous Descent Approach Methodology for Low Noise and Emission," *29th IEEE/AIAA Digital Avionics Systems Conference*, 2010, pp. 1.E.5-1–1.E.5-18.

[15] Turgut, E. T., Usanmaz, O., Canarslanlar, A. O., and Sahin, O., "Energy and Emission Assessments of Continuous Descent Approach," *Aircraft Engineering and Aerospace Technology*, Vol. 82, No. 1, 2010, pp. 32–38. doi:10.1108/00022661011028092

[16] Wei, W., and Hansen, M., "Impact of Aircraft Size and Seat Availability on Airlines' Demand and Market Share in Duopoly Markets," *Transportation Research Part E*, Vol. 41, No. 4, 2005, pp. 315–327. doi:10.1016/j.tre.2004.06.002

[17] Givoni, M., and Rietveld, P., "Airlines' Choice of Aircraft Size-Explanations and Implications," *Transportation Research Part A*, Vol. 43, No. 5, 2009, pp. 500–510. doi:10.1016/j.tra.2009.01.001

[18] Brueckner, J. K., and Zhang, A., "Airline Emission Charges: Effects on Airfares, Service Quality, and Aircraft Design, *Transportation Research Part B: Methodological*, Vol. 44, Nos. 8–9, 2010, pp. 960–971. doi:10.1016/j.trb.2010.02.006

[19] Lefebvre, S., Roblin, A., Varet, S., and Durand, G., "A Methodological Approach for Statistical Evaluation of Aircraft Infrared Signature," *Reliability Engineering and System Safety*, Vol. 95, No. 5, 2010 pp. 484–493. doi:10.1016/j.ress.2009.12.002

[20] Bilotkach, V., "Reputation, Search Cost, Airfares," *Journal of Air Transport Management*, Vol. 16, No. 5, 2010, pp. 251–257. doi:10.1016/j.jairtraman.2010.01.002

[21] Pai, V., "On the Factors that Affect Airline Flight Frequency and Aircraft Size," *Journal of Air Transport Management*, Vol. 16, No. 4, 2010, pp. 169–177. doi:10.1016/j.jairtraman.2009.08.001

[22] Martin, R. L., Oncina, C. A., and Zeeben, J. P., "A Simplified Method for Estimating Aircraft Engine Emissions," NASA CR-4700, April 1996; also *Scheduled Civil Aircraft Emission Inventories for 1992*, NASA, Washington, DC, pp. 13–15.

[23] Baughcum, S. L., Tritz, T. G., Henderson, S. C., and Pickett, D. C., "Scheduled Aircraft Emission Inventories for 1992: Database Development and Analysis," NASA Center for Aerospace Information Contract Rept. 4700, Hanover, MD, 1996.

[24] Sutkus, D. J., Baughcum, S. L., and DuBois, D. P., "Scheduled Civil Aircraft Emission Inventories for 1999: Database Development and Analysis," NASA Center for Aerospace Information Rept. NASA/CR-2001-211216, Hanover, MD, 2001.

[25] Lathasree, P., and Sheethal, R. M., "Estimation of Aircraft Fuel Consumption for a Mission Profile Using Neural Networks," International Conference on Aerospace Science and Technology, INCAST Paper 2008-115, Bangaloire, India, 26–28 June 2008.

[26] "User Manual for the Base of Aircraft Data (BADA)," Revision 3.8, 2010, http://www.eurocontrol.int/eec/gallery/content/public/document/eec/report/2010/007_BADA_User_Manual.pdf [retrieved 21 Sept. 2010].

[27] International Civil Aviation Organization, "Procedures for Air Navigation Services, Aircraft Operations, Vol. 2: Construction of Visual and Instrument Flight Procedures," 5th ed., 2006.